Published online: 2020-05-07

Organic Materials R. Otter, P. Besenius THIEME OPEN ACCESS Short Communication

Probing the Folding of Peptide–Polymer Conjugates Using the π-Dimerization of Viologen End-Groups

Ronja Otter[a]
Pol Besenius*[a]

[a] Department of Chemistry, Johannes Gutenberg University Mainz, Duesbergweg 10-14, 55128 Mainz, Germany
besenius@uni-mainz.de

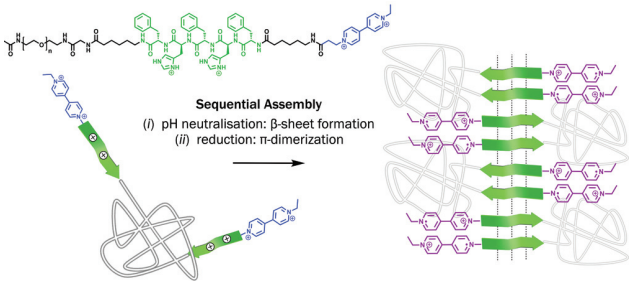

Received: 8.03.2020
Accepted after revision: 31.03.2020

DOI: 10.1055/s-0040-1710343; Art ID: om-20-0007-sc

License terms:

© **2020**. The Author(s). This is an open access article published by Thieme under the terms of the Creative Commons Attribution-NonDerivative-NonCommercial-License, permitting copying and reproduction so long as the original work is given appropriate credit. Contents may not be used for commercial purposes, or adapted, remixed, transformed or built upon. (https://creativecommons.org/licenses/by-nc-nd/4.0/).

Abstract The synthesis of a foldable viologen-functionalized peptide–polymer conjugate is presented. The ABA-type triblock conjugate with a PEG polymer was capped with a FHFHF pentapeptide sequence and further modified with a viologen building block at both chain ends. The pH-responsive peptide domains fold into an intermediate structure inducing close proximity of the viologen units, which upon a reduction step form π-dimers of the radical cation. Overall the intramolecular folding and intermolecular self-assembly process leads to the formation of supramolecular nanorods. Mixing of viologen-peptide–polymer conjugates with unfunctionalized conjugates leads to crosslinking of the nanorods and hydrogels with a tunable content of viologen end groups. π-Dimerization in the gels induces a deep purple color, which is used as an optical probe to monitor the diffusion of molecular oxygen through the hydrogel matrix.

Key words supramolecular materials, stimuli-responsive polymers, electrochromism, peptide conjugation, hydrogel

Introduction

The unique properties of viologens (di-quaternized 4,4′-bipyridyl salts), first mentioned by Michaelis in 1932,[1,2] have received much attention in the last few decades.[3,4] One of the most interesting properties is their stability in three different redox states. Viologens are prepared as dicationic species which show reversible redox behavior. The salts can be reduced by a one-electron reduction process and the resulting blue–violet colored radical cation is remarkably stable in the absence of oxygen, making it one of the most stable organic radicals. Upon further reduction, a neutral species is formed. The reversible one-electron reduction can be achieved chemically by reducing agents such as sodium dithionite,[5,6] electrochemically[7,8] or photochemically.[9–11] Some applications for viologen derivatives include the use in batteries[12–14] and in catalysis.[15–17] Based on the prominent reversible color change upon reduction, electrochromic devices[18,19] and dyes in solar cells have also been developed.[20] The above-mentioned properties have made viologens a popular building block in the field of supramolecular chemistry. Next to applications in the design of molecular machines, supramolecular host–guest type complexes with cucurbit[*n*]urils have been reported.[21–26] In some of these examples, the driving force of the radical cation to form dimeric species in solution is exploited. This so-called π-dimerization of the reduced viologen species represents an exciting noncovalent bonding motive and is therefore capable of triggering redox-responsive self-assembly and folding events.[27–32]

Our aim was to integrate the versatile viologen folding motive into peptide–polymer conjugates capable of secondary-structure-driven supramolecular self-assembly. Peptide–polymer conjugates combine the easy synthetic accessibility and scalability of hydrophilic polymers with the high structural definition and diversity of oligopeptides.[33–37] We have recently disclosed the synthesis of homo- and heterotelechelic peptide–polymer–peptide conjugates.[38,39] A hydrophilic polymer block of polyethylene glycol (PEG) or polysarcosine (PSar) was functionalized with an FHFHF pentapeptide sequence of alternating phenylalanine (F) and histidine (H) amino acids at both chains. In aqueous media the homotelechelic PEG and PSar conjugates exhibited the pH-responsive formation of anisotropic 1D nanorods due to a parallel β-sheet-encoded intramolecular folding and intermolecular self-assembly process. Concentrated solutions led to interstrand crosslinking and supramolecular hydrogel formation. Intriguingly, the heterotelechelic PSar conjugates with oligopeptide-directed antiparallel β-sheet domains also showed the formation of stable supramolecular nanorods.

However, no hydrogel formation could be observed, thus highlighting the susceptibility of these materials to small changes in the molecular structure. Here, we present the synthesis of a viologen-functionalized peptide–polymer conjugate in order to probe its β-sheet-encoded intramolecular peptide folding using the π-dimerization of redox-active viologen-labeled chain ends. The foldable multistimuli-responsive building blocks were further investigated in the formation of hydrogels, and the distinct purple color of the embedded radical dimers used as an optical probe for the diffusion of molecular oxygen. Our results pave the way for further developments and applications of the π-dimerization as synthetic bonding motive to induce sequential folding events in functional multidomain peptide materials.

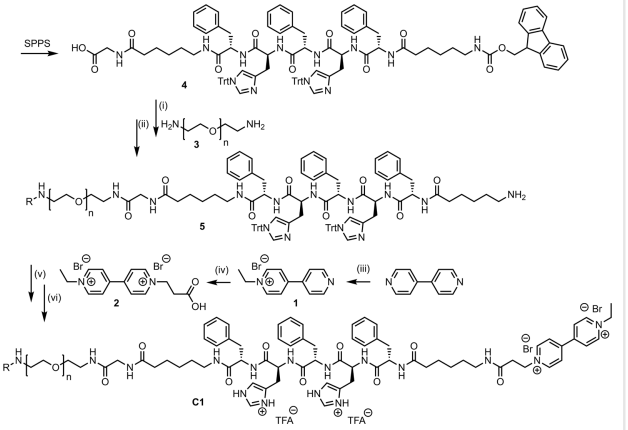

Scheme 1 Synthetic route to the viologen-functionalized peptide–polymer conjugate **C1** linked via C_6-spacers, utilizing a convergent approach: (i) PEG-3000 diamine **3** (X_n = 68, 1.0 eq.), **4** (2.3 eq.), PyBOP (2.3 eq.), HOBt (2.3 eq.), DIPEA (4.0 eq.), DCM, rt, overnight; (ii) DMF/piperidine (4:1), rt, 45 min (73% over 2 steps); (iii) 4,4′-dipyridyl (1.0 eq.), ethylbromide (10.0 eq.), benzene, 90 °C, overnight (59%); (iv) **1** (1.0 eq.), 3-bromopropionic acid (10.0 eq.), ACN, reflux, overnight (72%); (v) **5** (1.0 eq.), **2** (8.0 eq.), PyBOP (6.0 eq.), HOBt (6.0 eq.), DIPEA (6.0 eq.), DMF, rt, 24 hours; (vi) DMF/TFA/TIS/H_2O (20:20:1:1), rt, 45 min (96% over 2 steps).

Results and Discussion

In order to incorporate a viologen molecule into a peptide–polymer conjugate, 4,4′-dipyridine was functionalized with ethylbromide and 3-bromopropionic acid. The carboxylic-acid-functionalized viologen building block **2** could then be utilized in peptide coupling reactions. Similar strategies to modify peptides including the use of an active ester on a solid support have been described previously.[40,41] The β-sheet-encoded pentapeptide sequence FHFHF was flanked by two hydrophobic hexyl spacers to reduce steric congestion and shield the β-sheet domains in the resulting aqueous assembly process. Furthermore, the hexyl spacers should provide enough flexibility for both supramolecular motifs, the hydrogen-bonding peptide block and π-dimerization of the viologen radical cations, to function independently and thus in a sequential fashion. The trityl-protected peptide **4** was synthesized by conventional solid-phase peptide synthesis and cleaved from the resin under weakly acidic conditions using trifluoroethanol to leave the trityl-protecting groups on the histidine side chains intact. The N-terminal Fmoc-protected peptide was then used in a PyBOP/HOBt-mediated amidation to functionalize the diamine-modified PEG-3000 polymer **3** (X_n = 68). The N-terminus of the resulting homotelechelic peptide–PEG–peptide conjugate was straight away deprotected under basic conditions leading to the conjugate **5**. The viologen building block **2** was utilized to modify both chain ends of **5**, and after TFA-mediated deprotection of the imidazole side chains the viologen-functionalized amphiphilic peptide–polymer conjugate **C1** was obtained (Scheme 1).[42] The conjugate **C1** was purified by size exclusion chromatography (SEC) in methanol to remove excess of **2** and waste products from the coupling reagents. In addition, an acetamide-functionalized peptide–polymer conjugate **C2**, which lacks the viologen end groups, was prepared according to literature procedures (see the Supporting Information).[39] SEC characterization of **C1** in hexafluoroisopropanol (HFIP) revealed a significant reduction in the elution time compared to PEG diamine **3** (Figure S1). The SEC curves have a symmetrical shape, therefore indicating a unimodal molecular weight distribution, and the increase in molecular weight after conjugation was estimated using SEC calibration with PMMA standards[38,39,43] (31,000 g mol^{-1} for **C1** and 23,000 g mol^{-1} for **3**, Table S1).

UV/vis spectroscopy was first used to study the properties of the viologen moieties upon reduction to the radical cation. The spectra were measured in 10 mM degassed phosphate buffer at neutral pH values with sodium dithionite (1 mM) under an argon atmosphere. Sodium dithionite was added as a reducing agent. The process could be followed visually as the colorless solutions of the viologen dication (absence of absorption bands $\lambda > 300$ nm; Figures S2 and S3) turned blue in the case of a solution of **2** or purple in the case of **C1** upon reduction to the radical cation (Figure 1). The solutions were stable for hours in the absence of oxygen, but upon exposure to air, the oxidation led to the regeneration of the colorless dication species. The spectrum of a solution of **2** (100 μM) reveals a maximum absorption band at λ_{max} = 600 nm, as well as a weaker band at λ = 860 nm. In contrast, the spectrum of a neutral buffered solution of **C1** (100 μM) reveals a maximum absorption band at λ_{max} = 550 nm, but the band at λ = 860 nm is much more intense compared to that of the solution of reduced **2** (Figure 1). These observations are indicative of the π-dimerization of the radical cation in the case of **C1**. It has been shown previously

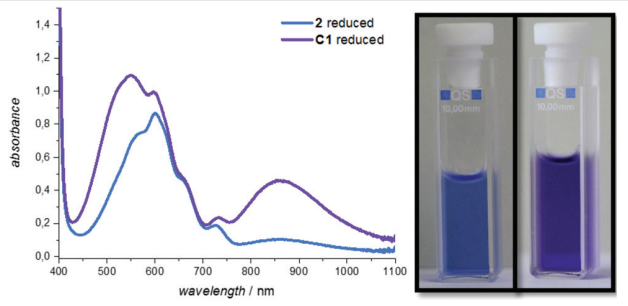

Figure 1 UV/vis absorption spectra of **C1** (100 µM) and **2** (100 µM) in 10 mM phosphate buffer at neutral pH after one-electron reduction using sodium dithionite (1 mM) and pictures of the colored solutions of **2** (left) and **C1** (right).

that the absorption band at λ = 860 nm is characteristic for the dimerization of the reduced radical cation.[27,44–46] The hypsochromic shift of the absorption band at λ = 600 nm provides further evidence for interactions between the radical cations in **C1**. We therefore suggest that at neutral pH, close proximity of the viologen end groups is provided due to the folding of hydrophobic β-sheet domains and supports π-dimerization of the reduced radical cation.

In order to confirm these first observations, we investigated the pH-responsive self-assembly behavior of the viologen-peptide–polymer conjugate **C1** and the impact of π-dimerization on the short-range order of the multi-segmented folding units. To this end, we conducted circular dichroism (CD) spectroscopy measurements of a 50 µM solution of **C1** in degassed 10 mM phosphate buffer (Figure 2). In acidic pH values a positive band at λ = 220 nm could be identified. After adjusting the pH value to pH = 8.5 and concomitant deprotonation of the imidazolium side

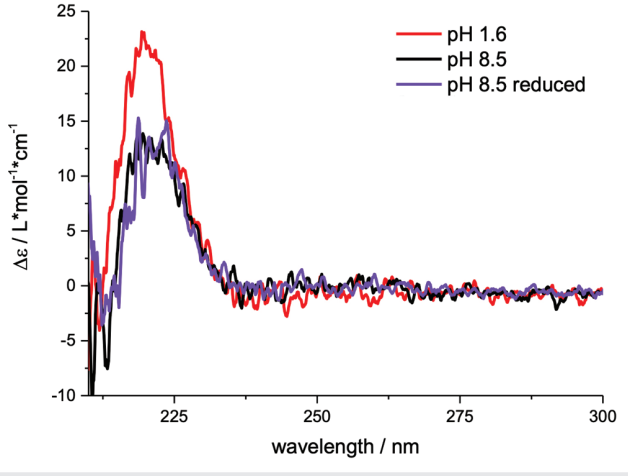

Figure 2 pH-dependent CD measurements of **C1** (50 µM) in 10 mM phosphate buffer (red and black lines) and CD measurement of **C1** (50 µM) after reduction with sodium dithionite (200 µM) in degassed 10 mM phosphate buffer (purple line).

chains,[47] a decrease of the CD signal at λ = 220 nm was observed (Figure 2). This observation is in agreement with our previous investigations using FHFHF- and FMHMHF-encoded oligopeptide–polymer conjugates that exhibit pH-responsive intramolecular folding and intermolecular self-assembly behavior.[38,39,43] The change in the CD signal intensity therefore indicates a change in the short-range order of the hydrophobic peptide domains of the viologen-peptide–polymer conjugate. In order to investigate the impact of the π-dimerization process upon reduction of the viologen units, we measured a solution of **C1** (50 µM) in degassed phosphate buffer (10 mM) with sodium dithionite (200 µM) at pH = 8.5. The CD band of the reduced species at around λ = 220 nm does not shift in intensity or energy, compared to the oxidized species. Based on the evidence from CD and UV/vis spectroscopic data, we conclude that the π-dimerization motive does not interfere with the β-sheet ordered segments of the multidomain conjugate **C1**.

The morphology of the self-assembled conjugate **C1** in the different states in aqueous solution was examined using transmission electron microscopy (TEM). For this purpose, **C1** (100 µM) was first dissolved in 20 mM Tris buffer at pH = 2.3. For measurements at neutral pH the solution was neutralized using a NaOH solution. The sample preparation for the reduced species was carried out under an argon atmosphere using a degassed solution to prevent fast oxidation by oxygen. All TEM images were negatively stained using a 2% uranyl acetate solution. Figure 3A shows a representative TEM micrograph of **C1** (100 µM) at pH = 2.3 displaying only small spherical objects. These micellar structures are most likely monomers or oligomeric assemblies. Due to the repulsive Coulomb interactions of the protonated histidine side chains at acidic pH, hydrogen-bond-driven directional self-assembly does not occur. In contrast, anisotropic supramolecular nanorods could be observed in TEM images prepared from aqueous solutions of **C1** at pH = 8.2 (Figure 3B). These structures are formed as a result of the intramolecular folding and intermolecular self-assembly process, supported by hydrophobic β-sheet domains at neutral pH values. TEM measurements of the sodium dithionite-reduced solution of conjugate amphiphile **C1** also reveal 1D supramolecular nanorods with similar contour lengths compared to the oxidized species (Figure 3C). This finding supports CD-spectroscopy experiments and radical dimer formation does not compete with the hydrogen bonding in the hydrophobic domains of the amphiphilic conjugate **C1**.

One exciting property of the viologen unit is its characteristic color changes, for example induced by the oxidation of the colored radical cation to the colorless dication species.[4] Although the radical cation is normally stable over long periods of time, the exposure to oxygen induces the oxidation via an one-electron transfer that results in the formation of the viologen dication and superoxide (O_2^{-}).[48,49] This property can be used as an optical device to detect the presence of molecular oxygen.[50–52] Due to our interest in developing adaptive

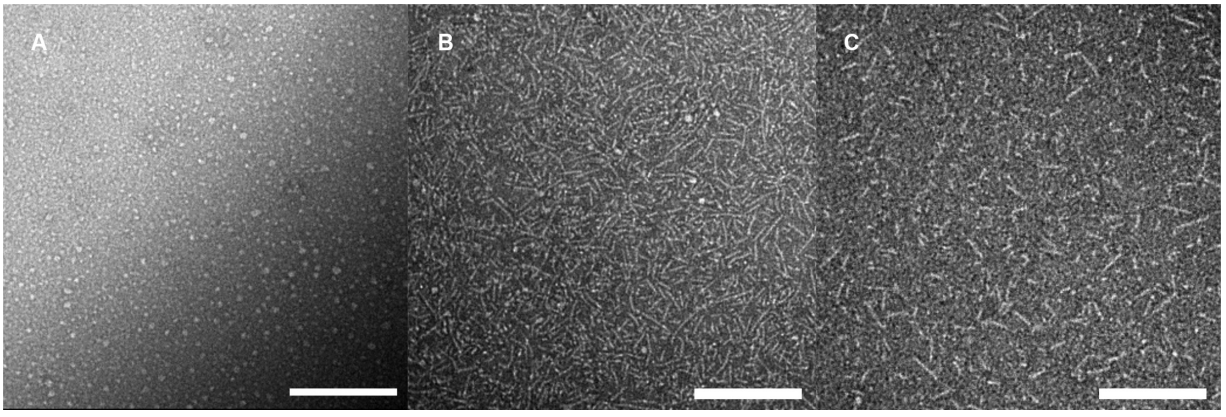

Figure 3 Negatively stained TEM Images: (A) **C1** (100 μM) in Tris buffer (20 mM, pH = 2.3). (B) **C1** (100 μM) in Tris buffer (20 mM, pH = 8.2). (C) **C1** (100 μM) reduced in Tris buffer (20 mM, pH = 7.4) with sodium dithionite (400 μM). Scale bars: 200 nm.

materials that respond to the presence of oxidative species and changes in redox microenvironments, we aimed to integrate the π-dimers as optical probes to monitor oxygen diffusion in supramolecular hydrogels. First, we performed hydrogelation experiments with **C1**, but neutral solutions of up to 3% (w/v) in degassed 10 mM phosphate buffer with sodium dithionite did not lead to stable hydrogel formation. The previously reported acetamide-functionalized peptide–polymer conjugate **C2**, which lacks the viologen end groups, is known to form gels at weight fractions as low as 1% (w/v) under the same buffered conditions.[39] We assume that in the case of **C1**, the hydrophobic peptide domains of the polymer conjugates are less likely to insert into neighboring nanorods due to the flanking π-dimerized radical cations. The reason is likely a combination of stabilization of the folded domains, steric hindrance, as well as Coulomb repulsion, which therefore reduces interstrand crosslinking and hydrogel formation. We therefore opted to mix both foldable synthons and added **C1** as a functional component to the structural gelator **C2**. **C1** (0.2 mM) and **C2** (2% w/v) were mixed and dissolved in degassed phosphate buffer (10 mM) at acidic pH under an argon atmosphere. After adjusting the buffer to neutral pH and the addition of sodium dithionite (0.8 mM), a dark purple supramolecular hydrogel was formed within minutes (Figure 4, first photograph). Note that the viologen building block is complementary to other electrochromic probes used in the literature, for example perylene diimide derivatives that show a strong driving force for self-assembly in the neutral state, but less so in the oxygen-sensitive reduced radical anionic states due to charge repulsion.[53–57] Using the described bicomponent hydrogels, it was possible to monitor the diffusion of molecular oxygen through the hydrogel matrix. To this end, the vial was opened after the gel was prepared and the argon atmosphere was replaced by blowing air into the vial. The transition from the purple radical cation dimer to the colorless dicationic viologen species becomes clearly visible as the oxidation reaction front propagates through the gel (Figure 4, second to fifth photographs). Over the time course of 3 h, all the viologen radical cations were oxidized and the hydrogel became completely colorless. Finally, this experiment was repeated using different weight fractions of structural hydrogelator **C2** (1.5% w/v and 2.5% w/v) to modulate the strength and mechanical properties of the hydrogels, while keeping the total amount of **C1** constant. In this concentration window, the oxygen diffusion and oxidation reaction seemed to occur on a similar time scale, and complete decolorization of the supramolecular hydrogels was observed after 3 h (Figures S4 and S5).

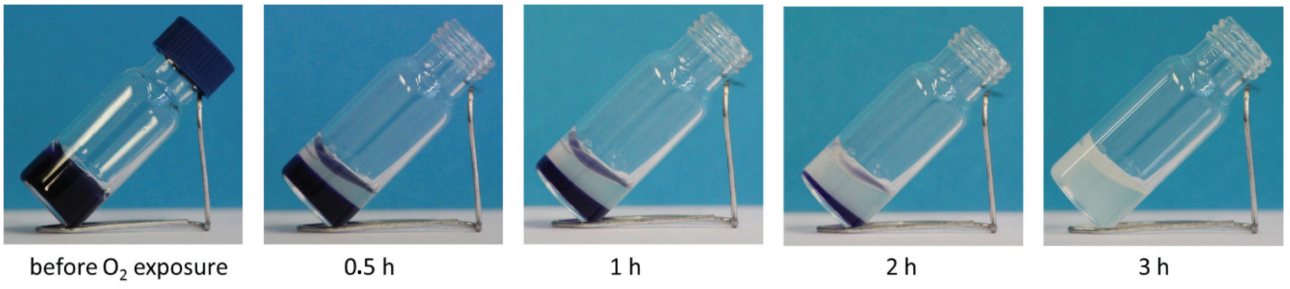

Figure 4 Hydrogel of **C2** (2% w/v) with **C1** (0.2 mM or 0.5% w/v) in 400 μL phosphate buffer (10 mM) and sodium dithionite (0.8 mM) under an argon atmosphere (left picture) and after exposure to air over time.

Conclusions

We present the facile synthesis of a homotelechelic ABA-type peptide–PEG conjugate functionalized with a viologen unit at both chain ends. The FHFHF pentapeptide sequence supports secondary-structure-driven self-assembly into supramolecular nanorods with a hydrophilic shell consisting of the water-soluble PEG polymer. The pH-switchable intramolecular folding and intermolecular self-assembly was characterized by CD spectroscopy and TEM experiments. The incorporation of the viologen units has no influence on the solution assembly properties, but prevents hydrogel formation of the amphiphilic peptide–polymer conjugate. UV/vis measurements revealed the formation of the purple-colored radical dimer, after a one-electron reduction of the viologen motives. This π-dimerization is favored due to the close proximity of viologen units in the folded state of the hydrophobic peptide domains. Finally, the redox-active conjugate was co-assembled with a similar but nonfunctional amphiphile to prepare bicomponent supramolecular hydrogels as optical probes for molecular oxygen. The diffusion of oxygen through the hydrogel matrix oxidizes the purple radical dimers and decolorization of the gel occurs with spatiotemporal resolution as the dicationic viologen is reformed. These findings and design features will inspire further developments for multidomain and multifunctional building blocks and their applications in noncovalent synthesis of supramolecular functional materials.

Funding Information

We acknowledge support from the DFG (CRC 1066).

Acknowledgments

We thank Lydia Zengerling for help with the MALDI-ToF experiments and Tobias Bauer (JGU Mainz, research group of Dr. Matthias Marz) for help with the GPC measurements and Prof. Dr. Opatz for providing access to the UV/vis spectrometer.

Supporting Information

Supporting information for this article is available online at https://doi.org/10.1055/s-0040-1710343.

References

(1) Michaelis, L. *Biochem. Z.* **1932**, *250*, 564.
(2) Michaelis, L.; Hill, E. S. *J. Gen. Physiol.* **1933**, *16*, 859.
(3) Striepe, L.; Baumgartner, T. *Chem. Eur. J.* **2017**, *23*, 16924.
(4) Ding, J.; Zheng, C.; Wang, L.; Lu, C.; Zhang, B.; Chen, Y.; Li, M.; Zhai, G.; Zhuang, X. *J. Mater. Chem. A* **2019**, *7*, 23337.
(5) Senn, D. R.; Carr, P. W.; Klatt, L. N. *Anal. Biochem.* **1976**, *75*, 464.
(6) Kameyama, A.; Nambu, Y.; Endo, T.; Shinkai, S. *J. Chem. Soc. D* **1992**, 1058.
(7) Thorneley, R. N. F. *Biochim. Biophys. Acta, Bioenerg.* **1974**, *333*, 487.
(8) Bird, C. L.; Kuhn, A. T. *Chem. Soc. Rev.* **1981**, *10*, 49.
(9) Kirch, M.; Lehn, J-M.; Sauvage, J-P. *Helv. Chim. Acta* **1979**, *62*, 1345.
(10) Borgarello, E.; Kiwi, J.; Pelizzetti, E.; Visca, M.; Grätzel, M. *Nature* **1981**, *289*, 158.
(11) Ebbesen, T. W.; Levey, G.; Patterson, L. K. *Nature* **1982**, *298*, 545.
(12) Janoschka, T.; Martin, N.; Martin, U.; Friebe, C.; Morgenstern, S.; Hiller, H.; Hager, M. D.; Schubert, U. S. *Nature* **2015**, *527*, 78.
(13) Janoschka, T.; Martin, N.; Hager, M. D.; Schubert, U. S. *Angew. Chem. Int. Ed.* **2016**, *55*, 14427.
(14) Hu, B.; DeBruler, C.; Rhodes, Z.; Liu, T. L. *J. Am. Chem. Soc.* **2017**, *139*, 1207.
(15) Wheeler, D. R.; Nichols, J.; Hansen, D.; Andrus, M.; Choi, S.; Watt, G. D. *J. Electrochem. Soc.* **2009**, *156*, B1201.
(16) Zhu, H.; Song, N.; Lv, H.; Hill, C. L.; Lian, T. *J. Am. Chem. Soc.* **2012**, *134*, 11701.
(17) Prier, C. K.; Rankic, D. A.; MacMillan, D. W. C. *Chem. Rev.* **2013**, *113*, 5322.
(18) Hwang, E.; Seo, S.; Bak, S.; Lee, H.; Min, M.; Lee, H. *Adv. Mater.* **2014**, *26*, 5129.
(19) Beneduci, A.; Cospito, S.; La Deda, M.; Veltri, L.; Chidichimo, G. *Nat. Commun.* **2014**, *5*, 3105.
(20) Boettcher, S. W.; Spurgeon, J. M.; Putnam, M. C., et al. *Science* **2010**, *327*, 185.
(21) Balzani, V.; Credi, A.; Raymo, F. M.; Stoddart, J. F. *Angew. Chem. Int. Ed.* **2000**, *39*, 3348.
(22) Kim, H-J.; Heo, J.; Jeon, W. S.; Lee, E.; Kim, J.; Sakamoto, S.; Yamaguchi, K.; Kim, K. *Angew. Chem. Int. Ed.* **2001**, *40*, 1526.
(23) Ong, W.; Gómez-Kaifer, M.; Kaifer, A. E. *Org. Lett.* **2002**, *4*, 1791.
(24) Badjic, J. D.; Balzani, V.; Credi, A.; Silvi, S.; Stoddart, J. F. *Science* **2004**, *303*, 1845.
(25) Moon, K.; Grindstaff, J.; Sobransingh, D.; Kaifer, A. E. *Angew. Chem. Int. Ed.* **2004**, *43*, 5496.
(26) Correia, H. D.; Chowdhury, S.; Ramos, A. P.; Guy, L.; Demets, G. J. F.; Bucher, C. *Polym. Int.* **2019**, *68*, 572.
(27) Zhou, C.; Tian, J.; Wang, J-L.; Zhang, D-W.; Zhao, X.; Liu, Y.; Li, Z-T. *Polym. Chem.* **2014**, *5*, 341.
(28) Kahlfuss, C.; Métay, E.; Duclos, M-C.; Lemaire, M.; Milet, A.; Saint-Aman, E.; Bucher, C. *Chem. Eur. J.* **2015**, *21*, 2090.
(29) Zhan, T-G.; Zhou, T-Y.; Lin, F.; Zhang, L.; Zhou, C.; Qi, Q-Y.; Li, Z-T.; Zhao, X. *Org. Chem. Front.* **2016**, *3*, 1635.
(30) Greene, A. F.; Danielson, M. K.; Delawder, A. O.; Liles, K. P.; Li, X.; Natraj, A.; Wellen, A.; Barnes, J. C. *Chem. Mater.* **2017**, *29*, 9498.
(31) Liles, K. P.; Greene, A. F.; Danielson, M. K.; Colley, N. D.; Wellen, A.; Fisher, J. M.; Barnes, J. C. *Macromol. Rapid Commun.* **2018**, *39*, 1700781.
(32) Kahlfuss, C.; Gibaud, T.; Denis-Quanquin, S.; Chowdhury, S.; Royal, G.; Chevallier, F.; Saint-Aman, E.; Bucher, C. *Chem. Eur. J.* **2018**, *24*, 13009.
(33) van Hest, J. C. M. Tirrell, D. A. *Chem. Commun.* **2001**, 1897.
(34) Klok, H. A.; Lecommandoux, S. *Adv. Mater.* **2001**, *13*, 1217.
(35) Vandermeulen, G. W. M.; Klok, H-A. *Macromol. Biosci.* **2004**, *4*, 383.
(36) Börner, H. G.; Schlaad, H. *Soft Mater.* **2007**, *3*, 394.
(37) Börner, H. G. *Prog. Polym. Sci.* **2009**, *34*, 811.

(38) Otter, R.; Klinker, K.; Spitzer, D.; Schinnerer, M.; Barz, M.; Besenius, P. *Chem. Commun.* **2018**, *54*, 401.

(39) Otter, R.; Henke, N. A.; Berac, C.; Bauer, T.; Barz, M.; Seiffert, S.; Besenius, P. *Macromol. Rapid Commun.* **2018**, *39*, 1800459 **Characterization of C2 ^{1}H NMR (400 MHz, DMSO-d_6, 298 K):** δ/ppm: 14.14 (s(br), 8H, NH_2^{+His}), 9.04–8.92 (m, 4H, CH^{His}), 8.48 (d, 2H, α-N*H*), 8.35 (d, J = 8.2 Hz, 2H, α-N*H*), 8.21 (d, J = 7.5 Hz, 2H, α-N*H*), 8.18–8.08 (m, 4H, α-N*H*/N*H*^{Ahx}), 8.03 (d, J = 7.4 Hz, 2H, α-N*H*), 7.99 (t, J = 5.6 Hz, 2H, NH ^{Gly}), 7.90 (t, J = 5.5 Hz, 2H, PEG-N*H*), 7.48–7.08 (m, 34H, CH^{His}/CH^{Phe}), 4.66–4.34 (m, 10H, α-C*H*), 3.65 (d, J = 6.0 Hz, 4H, CH_2^{Gly}), 3.50 (s (br), 264H, PEG–C*H*2), 3.39 (t, J = 5.8 Hz, 4H, PEGCH_2CH$_2$NH), 3.20 (q, J = 5.8 Hz, 4H, PEGCH$_2$CH_2NH), 3.11–2.70 (m, 24H, CH_2^{His}/CH_2^{Phe}/CH_2^{Ahx}), 2.10 (t, J = 7.5 Hz, 4H, CH_2^{Ahx}), 1.74 (s, 6H, NHCOCH_3) 1.50–1.40 (m, 4H, CH_2^{Ahx}), 1.36–1.26 (m, 4H, CH_2^{Ahx}), 1.19–1.10 (m, 4H, CH_2^{Ahx}). **MALDI-MS (DIT + KTFA, DCM/MeOH = 1/1) (m/z):** Calculated for $[C_{234}H_{391}N_{24}O_{83}]^+$: 4868.8, found: 4867.6; calculated for $[C_{234}H_{390}N_{24}O_{83}Na]^+$: 4890.8, found: 4890.0.

(40) Reczek, J. J.; Rebolini, E.; Urbach, A. R. *J. Org. Chem.* **2010**, *75*, 2111.

(41) Ogawa, M.; Balan, B.; Ajayakumar, G.; Masaoka, S.; Kraatz, H. B.; Muramatsu, M.; Ito, S.; Nagasawa, Y.; Miyasaka, H.; Sakai, K. *Dalton Trans.* **2010**, *39*, 4421.

(42) **Synthesis of C1**: **5** (295 mg, 49 µmol, 1 eq.) was dissolved in 2 mL DMF in a flask equipped with a stir bar. **2** (161.7 mg, 386 µmol, 8 eq.), PyBOP (100.9 mg, 193 mmol, 4 eq.), HOBt (26.1 mg, 193 µmol, 4 eq.), and DIPEA (53 µL, 290 µmol, 6 eq.) were added to the solution. The mixture was stirred for 6 hours at room temperature. Then PyBOP (50.4 mg, 96 mmol, 2 eq.) and HOBt (13 mg, 96 mmol, 2 eq.) were added to the yellow solution, which was stirred for 18 hours. Afterwards a mixture of TFA (2 mL), water (0.1 mL), and triisopropylsilane (0.1 mL) was added. The solution was stirred for 45 min at room temperature. After the deprotection, all volatiles were removed through reduced pressure and the solid was co-distilled with toluene. The residue was separated via size exclusion chromatography (Sephadex® LH 20, MeOH). **Yield:** 280 mg (47 µmol, **96%**) slightly yellow sticky solid. ^{1}H-**NMR (400 MHz, DMSO-d_6, 298 K):** δ/ppm: 9.43–9.38 (m, 8H, *H2*/*H6* ^{Viologen}/*H2′*/*H6′* ^{Viologen}), 8.81–8.77 (m, 8H, *H3*/*H5* ^{Viologen}/*H3′*/*H5′* ^{Viologen}), 8.50–7.97 (m, 20H, CH^{His}/α-N*H*), 7.91 (t, J = 5.7 Hz, 2H, α-N*H*^{PEG}), 7.45–7.11 (m, 34H, CH^{His}/CH^{Phe}), 4.90 (t, J = 6.4 Hz, 4H, N^{+}CH_2CH$_2$), 4.73 (q, J = 7.3 Hz, 4H, N^{+}CH_2CH$_3$), 4.66–4.41 (m, 10H, α-C*H*), 3.66 (d, J = 5.9 Hz, 4H, CH_2^{Gly}), 3.51 (s(br), 264H, PEG-CH_2), 3.40 (t, J = 5.8 Hz, 4H, PEGCH_2CH$_2$NH), 3.21 (q, J = 5.8 Hz, 4H, PEGCH$_2$CH_2NH), 3.11–2.74 (m, 28H, CH_2^{Ahx}/CH_2^{Phe}/CH_2^{His}), 2.10 (t, J = 7.5 Hz, 4H, CH_2^{Ahx}), 2.00-1.92 (m, 4H, CH_2^{Ahx}), 1.60 (t, J = 7.3 Hz, 6H, N^{+}CH$_2$CH_3), 1.47–1.42 (m, 4H, CH_2^{Ahx}), 1.32–1.23 (m, 12H, CH_2^{Ahx}), 1.18–1.11 (m, 4H, CH_2^{Ahx}), 1.02–0.94 (m, 4H, CH_2^{Ahx}).

(43) Otter, R.; Berac, C. M.; Seiffert, S.; Besenius, P. *Eur. Polym. J.* **2019**, *110*, 90.

(44) Iehl, J.; Frasconi, M.; de Rouville, H. P. J.; Renaud, N.; Dyar, S. M.; Strutt, N. L.; Carmieli, R.; Wasielewski, M. R.; Ratner, M. A.; Nierengarten, J. F.; Stoddart, J. F. *Chem. Sci.* **2013**, *4*, 1462.

(45) Wadhwa, K.; Nuryyeva, S.; Fahrenbach, A. C.; Elhabiri, M.; Platas-Iglesias, C.; Trabolsi, A. *J. Mater. Chem. C* **2013**, *1*, 2302.

(46) Iordache, A.; Kannappan, R.; Métay, E.; Duclos, M-C.; Pellet-Rostaing, S.; Lemaire, M.; Milet, A.; Saint-Aman, E.; Bucher, C. *Org. Biomol. Chem.* **2013**, *11*, 4383.

(47) Ahlers, P.; Frisch, H.; Holm, R.; Spitzer, D.; Barz, M.; Besenius, P. *Macromol. Biosci.* **2017**, *17*, 1700111.

(48) Farrington, J. A.; Ebert, M.; Land, E. J.; Fletcher, K. *Biochim. Biophys. Acta, Bioenerg.* **1973**, *314*, 372.

(49) Nanni, E. J.; Angelis, C. T.; Dickson, J.; Sawyer, D. T. *J. Am. Chem. Soc.* **1981**, *103*, 4268.

(50) Sweetser, P. B. *Anal. Chem.* **1967**, *39*, 979.

(51) Gong, Y-N.; Lu, T-B. *Chem. Commun.* **2013**, *49*, 7711.

(52) Tong, J.; Guo, X.; Jia, L.; Tian, X. *Mater. Lett.* **2015**, *158*, 255.

(53) Shirman, E.; Ustinov, A.; Ben-Shitrit, N.; Weissman, H.; Iron, M. A.; Cohen, R.; Rybtchinski, B. *J. Phys. Chem. B* **2008**, *112*, 8855.

(54) Baram, J.; Shirman, E.; Ben-Shitrit, N.; Ustinov, A.; Weissman, H.; Pinkas, I.; Wolf, S. G.; Rybtchinski, B. *J. Am. Chem. Soc.* **2008**, *130*, 14966.

(55) Schmidt, D.; Bialas, D.; Würthner, F. *Angew. Chem. Int. Ed.* **2015**, *54*, 3611.

(56) Leira-Iglesias, J.; Sorrenti, A.; Sato, A.; Dunne, P. A.; Hermans, T. M. *Chem. Commun.* **2016**, *52*, 9009.

(57) Leira-Iglesias, J.; Tassoni, A.; Adachi, T.; Stich, M.; Hermans, T. M. *Nat. Nanotechnol.* **2018**, *13*, 1021.